CODEN STJSAO
ZX470/1451

ISSN 0562-1887
UDK 531.717:621.397.42:528.73/.74

Flexible Multi-Camera Optical Surface Digitization System

Nenad DRVAR[1)], Stjepan JECIĆ[1)]* and *Mladen GOMERČIĆ[2)]

1) Fakultet strojarstva i brodogradnje, Sveučilište u Zagrebu (Faculty of Mechanical Engineering and Naval Architecture, University of Zagreb), Ivana Lučića 5, HR-10000 Zagreb, **Republic of Croatia**

2) GOM Gesellschaft für Optische Messtechnik mbH, Mittelweg 7-8, 38106 Braunschweig, **Germany**

nenad.drvar@fsb.hr

Keywords
Coded light method
Free form calibration object
Multi camera system
Shape digitalization
Uniqueness problem
Variable calibration parameters

Ključne riječi
Digitalizacija prostornog oblika
Metoda kodiranog svjetla
Problem jednoznačnosti
Slobodni kalibar
Sustav sa više kamera
Varijabilni parametri kalibracije

Received (primljeno): 2010-03-01
Accepted (prihvaćeno): 2010-04-30

Original scientific paper

Development of the flexible multi-camera optical surface digitization system which projects non coherent coded light in two perpendicular directions is presented. By the introduction of the absolute method for stereopairs indexing the need for twofold searching through the phase images is eliminated, as well as the influence of discontinuities. Critical areas responsible for outlier generation are eliminated prior to triangulation by combining the modulation filtering of phase images and gradient filtering of the absolute phase images. Sequential triangulation process enabled triangulation of points that are not visible in all the cameras, thus providing means for digitization of partially occluded areas. Free form calibration object eliminated the need for specialized planar calibration objects, which combined with variable external camera parameters resulted in a system that can be adjusted depending on the measurement problem. In comparison to the commercial single and stereo camera systems our approach reduces the number of projections for the digitization of the complete objects.

Fleksibilni optički digitalizacijski sustav s proizvoljnim brojem kamera

Izvornoznanstveni članak

Razmatrana je problematika razvoja fleksibilnog optičkog sustava s proizvoljnim brojem slobodnih kamera koji digitalizaciju oblika površine provodi dvostrukim projiciranjem nekoherentnog kodiranog svjetla. Apsolutnom metodom određivanja stereoparova eliminirana je potreba za dvostrukim pretraživanjem faznih slika, te utjecaj diskontinuiteta. Kombinacijom amplitudnog filtriranja slike parcijalnih faza i gradijentnog filtriranja slike apsolutnih faza eliminirana su kritična područja, te smanjen broj pogrešno identificiranih stereoparova. Uvođenjem slijednog postupka triangulacije omogućeno je trianguliranje i onih točaka koje nisu istovremeno vidljive u svim kamerama, odnosno uvedena je mogućnost digitalizacije površina djelomično zasjenjenih površinskim artefaktima. Kroz kalibraciju slobodnim kalibrom eliminirana je potreba za specijalnim planarnim kalibracijskim objektima, u sprezi sa varijabilnim vanjskim parametrima kalibracije sustav postaje prilagodljiv mjernom zadatku. U odnosu na komercijalno dostupne sustave s jednom i dvije kamere novi sustav omogućava smanjenje broja potrebnih projekcija za digitalizaciju kompletnog mjernog volumena.

1. Introduction

The request for shape information is historically associated with the measurement branch of mechanical engineering, but the need for the exact shape knowledge nowadays exists in a vast majority of industrial applications. For example, shape information is important for the accurate position check [1], modeling of sheet forming moulds and the elastic return control, for shortening of the development time through clay modeling in automotive industry, car airflow CFD analysis or the numerical damage simulations, quality control or reverse engineering. Even body deformations and displacements can be considered as the comparison of deformed and undeformed shape. During the last decade optical measuring systems have started to take over in shape control processes, where traditional CMMs have been used. Regarding the measurement point definition, digitization systems can be classified as passive (without projector) and active systems. Unlike active systems, passive systems cannot use a single pixel in the image as the measurement point. In order to correlate two or more images, passive systems need to find the same area in the image domain, so they also need to take into consideration certain area around the reference pixel. This leads to inability of digitization of discontinuous or rough surfaces, the area around the edges or areas with a small radius of curvature. This paper is based on the development of the active projection system; the analysis of passive systems is in progress,

Symbols/Oznake

p, p´	- stereopair coordinates, pixel - koordinate stereoparova
F	- fundamental matrix - fundamentalna matrica
H	- homography matrix - matrica homografije
R	- coordinate system rotation matrix - matrica rotacije koordinatnog sustava
c	- camera constant, pixel - konstanta kamere
I	- pixel intensity - svjetloća piksela
X, Y, Z	- object coordinates, mm - objektne (prostorne) koordinate5
X_0, Y_0, Z_0	- lens center coordinates, mm - koordinate projekcijskog središta objektiva
φ (*x, y, t*)	- referent phase - referentna faza
δ (*x, y, t*)	- partial phase - parcijalna faza

Indices / Indeksi

i	- object point index - indeks objektne točke
j	- camera index - indeks kamere

under the assumption that the effects of camera and image processing for both types of systems with more than two cameras will be similar. Direction of active systems development that is nowadays used for the non contact shape digitalization of the static objects started parallel to the development of the personal electronic computers, by development of a single camera and projector in the convergent setup. By active projection systems, we consider measurement systems that define unique position of the spatial point on the surface of the measurement object by projecting some sort of coded light patterns. A measuring point is determined relative to the current global coordinate system of the measurement system, not the measured object. The role of the projector is to unambiguously define the relative position of each measuring point on the surface of the measuring object. Reconstruction of spatial coordinates by means of triangulation is based on the analysis of pixel intensity recorded by digital camera. This setup required that relative camera orientation to the projector is known, along with the correction of the eventual influences of the optical elements on the deformation of the recorded images. Procedures needed to determine parameters of the mathematical model for the photogrammetry based systems are known as the system calibration, and are usually conducted by using the special calibration objects of known size or displacement. This step is necessary for the process of determination of the parameters which describe orientation of system elements, which are needed for extracting 3D information from 2D images. Some authors use specific calibration objects with the controlled or general displacements [2-5], and those procedures lack standardization. Calibration objects are usually planar objects of known geometry (adapted to the required measurement volume and the available optical elements). During the calibration stage the absolute rigidity of calibration objects is assumed. After the system was calibrated, the relative orientation camera – projector was not supposed to be altered because single camera systems did not have the instrument to detect decalibration from the information available during the measurement process. Calibration object's finite sizes, production accuracy, together with the accuracy of displacements were in direct relation with the expected measurement accuracy and resolution of the measurement system. Further improvement was the addition of second camera. The uncalibrated projector role is now reduced to providing assistance for solving the uniqueness problem. The projector is usually positioned centrally between the camera pair. The additional camera allows recording of total of four image coordinates of each coded spatial point (spatial point is determined by three coordinates), thus eliminating the need for projector calibration. Some commercial systems still allow projector calibration, if needed; two-camera system can thus reduce to two single camera systems. Reconstruction of the spatial location of the observed object point is conducted by triangulation process; where for each image point per camera one virtual light beam is projected back into space. A point in space where those beams meet is considered to be the reconstructed spatial point position. Depending on the camera model, rigidity of the system and influence of the object surface, those beams might not intersect. In that case the measurement point is usually positioned at the midpoint of shortest distance between beams. In order to conduct triangulation procedure, a stereo system needs to know the relative orientation of the utilized cameras (external calibration parameters), as well as the parameters which describe the geometry of the optical elements of the camera and their influence on the distortion of the recorded image (internal calibration parameters). Stereo camera systems can simplify the uniqueness problem of finding the same image point in both cameras by exploiting known geometry information. Even for the

case of unknown system geometry it is possible to use epipolar principle by looking at the way a plane placed through camera centers and image point intersect with a second image. Calibration objects are still mostly planar [6-12], and use special surface markings of known geometry. Compared to single camera systems, identical limitations regarding frame rigidity are valid for stereo camera systems. Both system types assume that internal and external calibration parameters remain the same after calibration procedure is performed. Any deviation from this assumption will lead to systematic errors which cannot be quantified during the measurement process (e.g. scale change) [13-14]. Frame rigidity is influenced by many external and internal factors, e.g. heat from the lamp, vibrations from built in fan or tripod stability. Taking into account the need for mobility and the need for shape measurement in the industrial environments this can be one of factors that limits system versatility. If one would like to change measurement volume in-situ, it would be necessary to conduct system recalibration by using the appropriate calibration object. Some of the commercial systems avoid heat and vibration effects by using a separate light source which is connected to the system via fiber optic cable. If a fan is used to cool the built in light source, this means that one of the vibration sources is built directly into sensor body. In this discussion we did not focus on the type of projected light because we assumed that projectors are not calibrated and are used just for solving the uniqueness problem. Equivalent discussion would be valid for systems that project monochromatic laser light and on systems that project white light that code measuring point by means of projecting geometrically regular or irregular pattern that produce code which changes in time. Development of the next generation of digitalization systems with arbitrary number of cameras [15-16], based on modification of ATOS stereo camera system, is presented in this paper. Modified projection approach [15, 17] eliminates the need for the epipolar geometry during the uniqueness problem solving because now each point on the surface of measured object has two different phases. In order to identify stereopairs it is not necessary to know the exterior calibration parameters or fundamental matrix. It is also not necessary to triangulate spatial points based on geometry obtained by initial calibration because bundle adjustment allows us to conduct the entire procedure consisting of calibration and measurement in the same step. Stereo camera systems utilized epipolar geometry to reduce search domain in second image, because a sought seeked pixel is supposed to lie on a line defined by the intersection of epipolar line and image plane in the second camera. The need for the elimination of epipolar geometry dependency leads to the need for searching within two absolute phase images per camera. We investigated the possibility of improving indexing speeds by computing the unique absolute phase, per pixel. Discontinuities exhibited a special problem in the search process because they lead to errors in search, or to occlusions. Erroneous stereopairs can be visible after triangulation as outliers in the space around the actual measurement data. One of the common elimination procedures is the utilization of statistical analysis for eliminating points whose deviation exceeds the allowed measurement noise. That is not the ideal solution because the overall deviation is also calculated based on wrong data provided by those outliers. Since stereopair identification is a process that precedes triangulation, it would be beneficial to eliminate possible outliers in this step. That way convergence of the mathematical model would speed up, at the same time the overall point deviation would be reduced. We implemented the new mechanism for outlier detection and elimination in the phase image domain, preceding triangulation. Contrary to contact measurement methods that can require large dimensions and rigidity of measurement system, optical systems due to their relatively small mass should be able to adapt to the measurement problem, which would make them extremely practical in everyday exploitation. This would be possible if the frame were to allow free camera placements, so we investigated the possibility of varying external calibration parameters during the measurement process. Contact CMMs have the possibility of direct calibration on a reference model, which provides more consistent calibration in the actual working volume. Here we showed that new system can also be calibrated with free-form object (even measurement object can be used for calibration), thus improving both adaptation to the measurement problem and stability of mathematical model.

1.1. New system requirements

Development of a new projection system seeks to create the backbone for a new generation of open and flexible system, which, compared to current stereo systems involves simple addition and easy calibration of arbitrary number of cameras. Therefore, when choosing a mathematical model, the following guidelines for developing the system with multiple cameras were followed. Requirements of the new system (Figure 1):

- it has to use three or more cameras,
- it has to have variable external calibration parameters,
- it should use each pixel in camera as a separate measuring point,
- it should be able to adapt calibration to the measuring object,
- it should have possibility of self calibration,
- it should have reduction of number of projections compared to single and stereo camera systems,
- it should make improvement of spatial resolution and surface detail digitization,

- digitization of partially occluded surfaces,
- ability to link multiple projections in a point cloud,
- simplification of the measurement planning process.

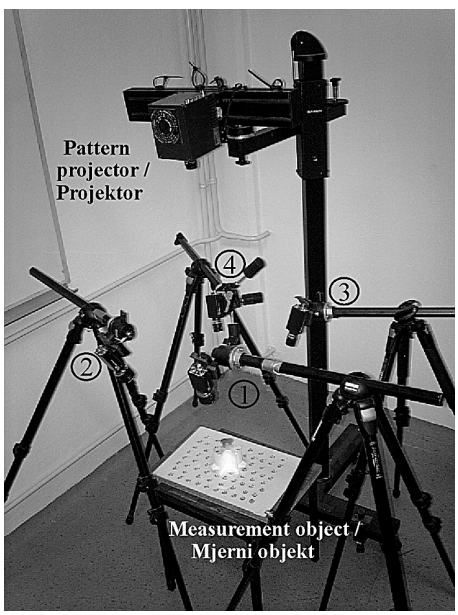

Figure 1. Four camera system setup
Slika 1. Postav novog mjernog sustava

1.2. Description of the measurement procedure

Optical measurement procedures (Figure 2) usually consist of the following steps, common to all versions of optical digitization systems regardless of the number of cameras used and the type of projected pattern:

- preparation of the measuring object,
- configuration of optical elements of the projector and cameras,
- determination of internal and external parameters of the selected mathematical model with the calibration process,
- solving the uniqueness problem by coded light pattern projection,
- triangulation of object coordinates,
- joining the measurement results from different orientations of the measuring object,
- visualization and processing of results.

2. Mathematical model

2.1. Bundle adjustment method

This method of determining the relative orientation of the camera - measuring object is based on the calculation of adjustment of deviations of the predefined system of equations, for each of the cameras consisting of equations 2 and 3. Since each camera is modeled separately, this method is suitable for introduction of more than two cameras in the projection measurement systems. Relative orientation of cameras is computed under the assumption that the observed object during the calibration process

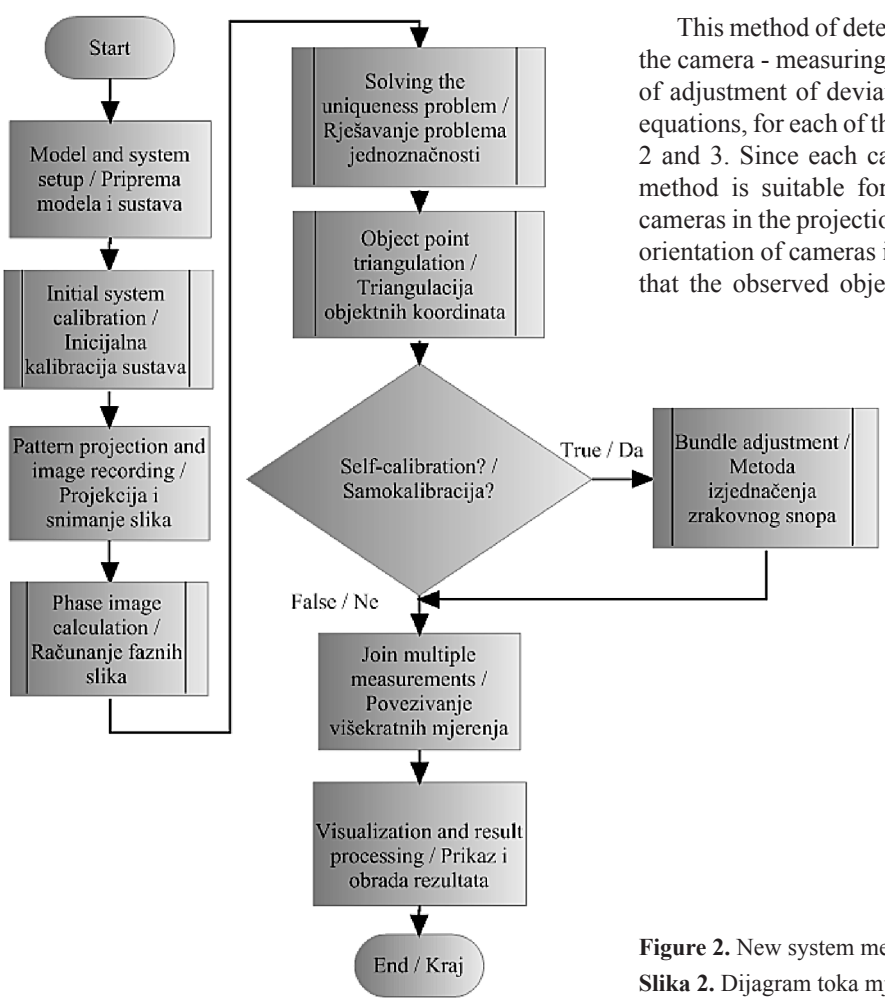

Figure 2. New system measuring principle flow chart
Slika 2. Dijagram toka mjerne procedure novog sustava

keeps an unchanged geometry, and has the appropriate markers required for solving the uniqueness problem. Recording of the marked surface of the calibration object can be carried out from various orientations with one or more nearly identical cameras. The method principle will be explained on a model of ideal pinhole camera [18-20], without parameters that describe lens aberration influences. Based on a colinearity of lens center point *O* and the spatial object coordinate of a point *P* (Figure 3), we can relate image coordinates with spatial object coordinates:

$$\begin{bmatrix} X \\ Y \\ Z \end{bmatrix}_i = \lambda_{ij} R_j \begin{bmatrix} x_{ij} - x_{0j} \\ y_{ij} - y_{0j} \\ 0 - c_j \end{bmatrix} + \begin{bmatrix} X_0 \\ Y_0 \\ Z_0 \end{bmatrix}_j . \quad (1)$$

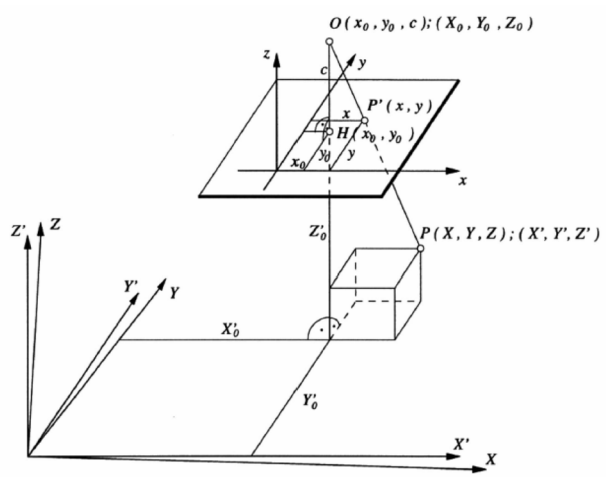

Figure 3. Camera projection model
Slika 3. Projekcijski model kamere

Where index *i* relates to the ID of the observed spatial point, while index *j* relates to the camera used (or image ID if all the images are recorded by a single camera from multiple orientations). If we dismember eq. 1 so that the left of the equation sign are image coordinates, and λ_{ij} omitted, the relation between image and object coordinates is given by:

$$x_{ij} = -c_j \frac{r_{11j}\left(X_i - X_{0j}\right) + r_{21j}\left(Y_i - Y_{0j}\right) + r_{31j}\left(Z_i - Z_{0j}\right)}{r_{13j}\left(X_i - X_{0j}\right) + r_{23j}\left(Y_i - Y_{0j}\right) + r_{33j}\left(Z_i - Z_{0j}\right)} + x_{0j} \quad (2)$$

$$y_{ij} = -c_j \frac{r_{12j}\left(X_i - X_{0j}\right) + r_{22j}\left(Y_i - Y_{0j}\right) + r_{32j}\left(Z_i - Z_{0j}\right)}{r_{13j}\left(X_i - X_{0j}\right) + r_{23j}\left(Y_i - Y_{0j}\right) + r_{33j}\left(Z_i - Z_{0j}\right)} + y_{0j} . \quad (3)$$

Components $r_{11j} \ldots r_{33j}$ represent the elements of the rotation matrix.

Bundle adjustment model can be applied to general photogrammetric problems that can be distinguished as:

- a general problem in which all parameters on the right side in equations 2 and 3 are unknown,
- determination of external calibration parameters, if internal are known (e.g., orientation of metric cameras);
- internal orientation and coordinates of object points are known, the external orientation parameters are computed;
- ehere only the coordinates of object points are known, it is necessary to determine the parameters of internal and external orientation;
- parameters of internal and external orientation are known; the coordinates of object points can be calculated.

3. Solving the uniqueness problem

In order to digitize one of the object states, measurement images should be recorded with overlap, from different locations in space around the object. Point triangulation requires stereopairs (pairs of image points that represent the observed object point) to be known in all the recorded images. Recognition of image points which belong to the same observed object point in two or more images of the same object is known as the uniqueness problem. It occurs regardless of the system calibration state. Motivation for solving the uniqueness problem is to enable both the system calibration and point cloud triangulation on the entire surface of the measured object. Each stereopair can consist of a single pixel or a group of pixels. It will be successfully found under the condition that in each image the same group of pixels can be identified only once. Ideally, an image point would be defined by a single pixel, thus discrediting the object surface by the smallest possible image element. Active projection systems have the advantage of separately coding each pixel, which is a reason for their usage in this work. Surface occlusions and local discontinuities can additionally complicate finding stereopairs because part of the model can accidentally hide another part in the second camera, making it invisible for the second camera even though it was correctly indexed in the first camera. Systems that use two cameras are mostly used in today commercial systems but they suffer from this effect, which motivated development of the multi camera system presented in this paper. Generally, the projection systems solve the uniqueness problem by combining two principles: by taking advantage of known information about the geometry of the measuring object and the camera system, and varying the pattern projected onto the surface of the measuring object.

3.1. Geometric over determination

The known system and object geometry can be utilized for accurate or approximate stereopair locating. They are

not always known, e.g. the system is not yet calibrated or nothing is known about the object to be measured. In some cases plane homographies and methods based on the epipolar plane can be used as an additional tool for the uniqueness problem solving. Plane homographies are projection transformations which describe how single point projects from plane to plane, eq. 4.:

$$\mathbf{p}' = \mathbf{Hp}. \quad (4).$$

By using eq, 4, we can describe how point *P* projects from plane in object space to point *p* in the image plane, or its projection from one image plane to the other image plane ($p \Leftrightarrow p'$) , Figure 4. It is necessary to know the homography matrix **H**, which can be determined under condition that the observed object is locally planar and of known shape, providing that information about system calibration is known.

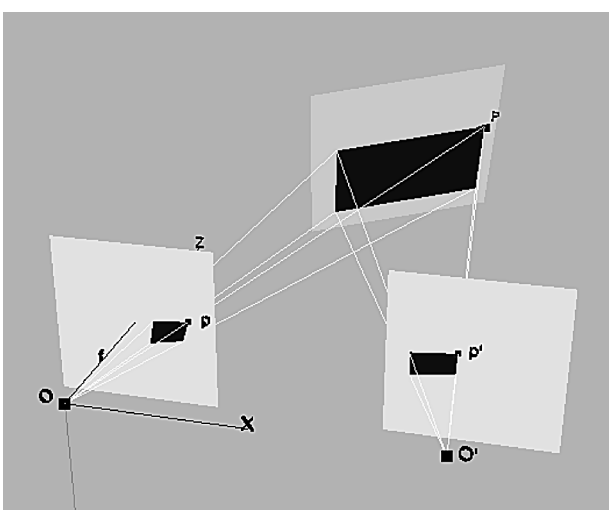

Figure 4. Plane homographies

Slika 4. Ravninske homografije

Calibration also requires the ability to solve the uniqueness problem, and to know piecewise object geometric information, but they are usually not known. Point to point transformation would provide direct instrument to solve the uniqueness problem but since the assumption of the local surface planarity assumes observation of a pixel group, plane homographic approach does not provide sufficient information for the active projection systems. However, it can be used with the passive systems where local planarity assumptions apply (e.g. in surface deformation measurements [21]).

$$\mathbf{p}^{\mathrm{T}}\mathbf{Fp}'. \quad (5)$$

Based on the eq. 5, epipolar approach defines projection of image point *p* from one image plane to line *l'* in second image plane, Figure 5. It is done by constructing a plane between image centers and the object point (shaded triangle in Figure 5), but their relative orientation does not need to be known in advance. Compared with piecewise unique solutions provided by homographic approach an epipolar approach does not completely solve the uniqueness problem. The advantage is that no assumptions regarding geometric properties of the observed model are needed for the fundamental matrix computation (only that geometry of both object and system is not changed during the image recording stage). This provides uniqueness problem generalization regarding the measured object geometry, but considering the request for the variable external calibration parameters of the new system, rigidity of camera setup makes this method still somewhat limited. If an operator changes some of the external or internal calibration parameters of the stereo system during the measurement process, it will reflect as a systematic error that is in some cases impossible to detect because parameters of the essential and fundamental matrix were determined by the initial system calibration. Literature brings variation of epipolar geometry principle for three and four cameras, but those methods do not provide a simple mechanism for adding or removing cameras from the system, with similar limitations as the epipolar stereo system approach.

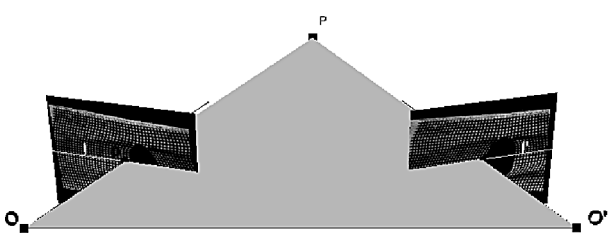

Figure 5. Epipolar geometry

Slika 5. Epipolarna geometrija

3.2. Projection pattern

Development of the LCD projectors enabled extremely simple testing of the various projection patterns. Patterns are used as an instrument to identify stereopairs in each of the recorded images. It is common to all the projection patterns that they try to assign the unique numerical ID to each pixel (or pixel group). Position and numerical ID of a coded pixel will depend on the type of projected pattern, but also on the analysis type, e.g. coding by monochromatic intensity, color or by projection of pattern of a know geometric shape. There are many coded light methods which can be summarized according to [22] in three categories: time coding, object coding and direct coding. Direct codification strategy projects a pattern that is defined in such a way that a single projection is sufficient to code each image pixel, e.g. such color coding that each pixel or each line of pixels has a different color. It is extremely sensitive to the projector and camera linearity and to a change of the ambient lightning because projected

sample definition can appear different in the recorded image because of the interaction with local color of the surface of the observed object. It is not applicable in the sensitive measurement tasks because of the high amount of noise. Object coding of the measurement information is based on a projection of a single pattern that consists of structures whose geometry and intensity distribution is known in advance. Single projection allows it to be used in dynamical measurements. Object coded pattern can be of pseudorandom or exactly known shape, e.g. De Brujin pattern or dashed parallel lines. Reconstruction of a measurement information for a single pixel has to be conducted based on a group of neighboring pixels (often called facets), which is one of the disadvantages of object projection strategies because it makes it difficult to scan surfaces that have big curvatures or edges and discontinuities. The advantage is in direct uniqueness problem solving, since the pattern is often coded in such a way that a certain group of pixels will appear in image only once. The third group of codification strategies projects various pattern slides sequentionaly. Each of the pattern slides is defined in such a way that if an analysis is conducted not in image domain like previous methods, but in the time domain, a unique coding of each pixel can be obtained. This enables the analysis of each pixel separately to its neighbor, which contributes to method robustness. It avoids error propagation because it does not consider the neighboring pixels. High spatial resolution can be achieved by analyzing each pixel for itself. The pattern is generally very simple, usually consisting of binary coded parallel stripes. Due to the need for projecting series of slides in time, this method is not suitable for dynamical measurements. A modified version of combination of phase shift and Gray code projection is used in the new system, by projecting it in two perpendicular directions. A basic model and introduced modification will be here presented in greater detail. If we define light intensity of a single pixel in the image plane I as:

$$I(x,y,t) = s(x,y,t) + a(x,y,t) \cdot \cdot \cos\left[\delta(x,y,t) + \varphi(x,y,t)\right], \tag{6}$$

where s(x,y,t) is the mean overall intensity for some pixel, a(x,y,t) modulation, δ(x,y,t) for each pixel uniquely defined phase and φ(x,y,t) additional reference phase. During statical object measurements unknown parameters s(x,y,t), a(x,y,t) and δ(x,y,t) for all the image pixels actually do not depend on time, because changing time duration between projection of each slide does not change the intensity of each pixel for a given slide. These parameters can be considered as a function of the projector and the projected pattern whose controlled displacement φ(x,y,t) is changed. In order to find those three unknowns we need to record a minimum of three images, but to minimize noise it is common to use over defined system with four or more projected patterns. In a case of four phase images, δ(x,y) can be expressed as:

$$\delta(x,y) = \arctan\frac{I_2 - I_4}{-I_1 + I_3}. \tag{7}$$

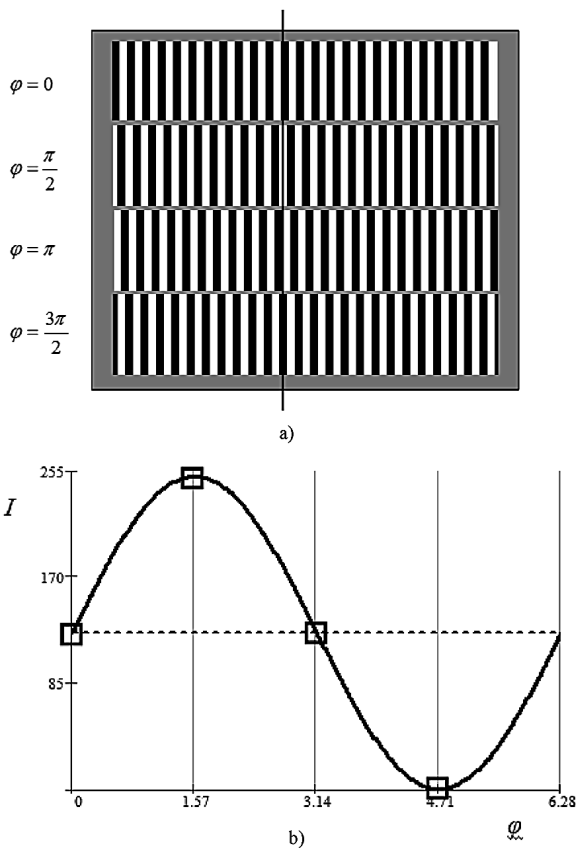

Figure 6. Phase shifting principle: a) projected pattern shifted by $\pi/2$, b) controlled light change of the observed pixel

Slika 6. Princip metode vremenskog faznog pomaka: a) projicirani uzorci pomaknuti za $\pi/2$, b) prikaz kontrolirane promjene osvijeljenosti u nekom pikselu

Phase shift principle will be explained by simulating projection on a flat plane and recorded by a left camera of two camera system. Four projections of the same pattern, each shifted by $\pi/2$ are illustrated by Figure 6a. The projected pattern consists of parallel black fringes followed by equally wide white ones. Edges between fringes are in this example sharp, but for the actual measurements phase noise will be lower if the grating is sinusoidal in horizontal direction. If we assume that pattern is projected parallel to pixels in camera, and that in this example phase shift is introduced to the right, then vertically stacked projected stripe samples show how the intensity of each pixel changes in time. Intensity variation for a given pixel in time is defined by a vertical cross-section of Figure 6a. A given pixel in the first projection observed in the left image is located on the

edge of projected lines. In a second projection shifted by $\pi/2$ that pixel is completely white, followed by another projected edge and a completely dark stripe during the last projection. If 8-bit camera was used, completely white pixel had intensity of 255 and completely dark pixel 0. In our example, the pixel in the first slide will have an intensity about 128, in second slide shifted by $\pi/2$ intensity will be 255, then 128 and finally 0, which is illustrated by squares Figure 6b. If we fit equation 6 through these points, resultant position of the entire sinusoidal curve is a partial phase for a given pixel, calculated by the eq. 7. If measurements were carefully conducted, and both camera and projector were linear, then mean value and modulation should be unified over the entire image. Figure 6b should look the same for a neighboring pixel, slightly shifted in phase. Shift direction depends on the direction of the projected pattern shift; the amount depends on how far the observed pixel is to the referent one.

Due to the repeating nature of projected pattern, pixels with the same repeating codes will exist on the pixels separated by one black and one dark fringe. This will result in the saw tooth like partial phase image (Figure 7a) with the apparent repeating pattern (taken from the actual measurement). The repeating effect disables the unique identification of a certain phase in the right image, because partial phase value repeats multiple times across the horizontal row of pixels, as shown by Figure 7b.

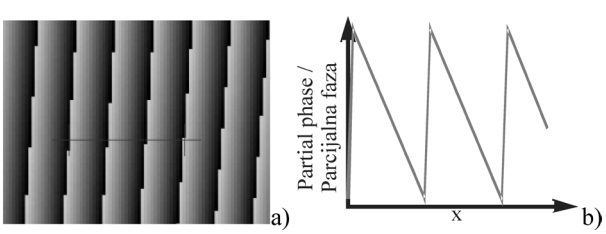

Figure 7. Detail of a) partial phase distribution, b) saw tooth phase distribution.

Slika 7. Detalj a) parcijalnih faza na površini objekta, b) pilasti uzorak uzduž horizontalnog presjeka.

In order to solve this additional uniqueness problem, for the absolute phase calculation, the binary stripe projection coded by Gray code principle is used. The method is based on the consecutive thickening of the projected lines. By the careful projection of six patterns [16] the area where each "tooth" of the partial phase is defined is coded by a combination of light and dark fields, resulting in stair-like Gray code image (Figure 8a) where the width of the each stair corresponds to the width of the phase tooth. The height of the each stair is a multiple of 2π, Figure 8b.

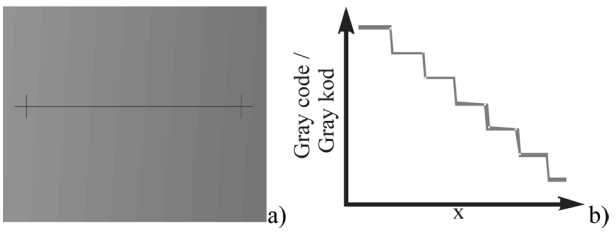

Figure 8. Detail of a) Gray code distribution, b) stair-like phase distribution

Slika 8. Detalj a) Gray koda, b) stepenaste raspodjele osvijetljenosti

Reconstruction of the absolute phases (Figure 9) in the next step is reduced to the sequential summation of partial phases (saw-tooth image) with Gray code stair-like image. It has to be done for each pixel, in each image separately. The absolute phase associated with each pixel is reconstructed independently from its neighbors, thus reducing the error in locating position of neighboring areas. Stripe projection results in the absolute phase image where phases repeat in the vertical direction (in the ideal setup), in real setups they are almost vertical as seen in Figures 7 and 8. The uniqueness problem is not entirely solved because the same absolute phase still repeats in the vertical direction (in image 9 marked with vertical lines). Systems consisting of two cameras and a projector thus need to exploit their geometric over determination. Stereopair is defined as a cross-section of the line consisting of the observed absolute phase and epipolar line in each image, as illustrated by Figure 9. Geometric dependency results in stereopair that is not independently located in both cameras, which motivated development of double projection of the explained pattern, but in two mutually perpendicular directions.

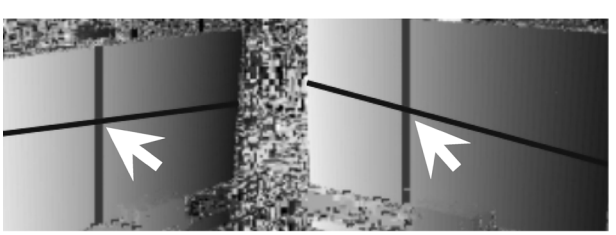

Figure 9. Absolute vertical phase distribution for a planar specimen, shown in both cameras

Slika 9. Apsolutne vertikalne faze na ravnoj plohi u lijevoj i desnoj kameri

This results in pixels that are coded twice. All recorded pixels now have two independent absolute phases, horizontal and vertical. Based on the assumption that during the projection of vertical and horizontal pattern there was no movement between projector, cameras and model, because of double indexing it is not necessary to use epipolar geometry to find stereopairs. In order

to find its stereopair in the second image, it should be sufficient to find the pixel with an equal combination of horizontal and vertical phase. This approach combines the advantages of phase shift methods with the absolute solutions provided by direct coding strategies. Image coordinates of stereopairs are now independently coded, and they can be compared to the passive markers in the traditional photogrammetry, while contributing to the over determination of the triangulation model. This modification enables the application of bundle adjustment method during the measurement process in order to triangulate object points. Previously, bundle adjustment was mainly used during the calibration stage. Camera calibration can be additionally optimized during the measurement, thus incidentally compensating eventual changes in calibration parameters resulting in the influence of the external sources (e.g. by the environmental temperature changes, vibrations).

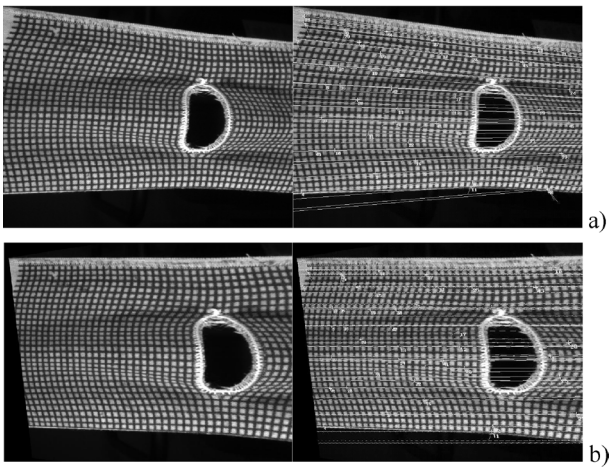

Figure 10. Example of image rectification, a) original image, b) rectified image with epipolar lines shown

Slika 10. Ilustracija rektifikacije sa ucrtanim epipolarnim linijama a) originalna lijeva snimka, b) rektificirana

4. Stereopair tracing

In the ideally parallel stereo camera setup, stereopairs in both cameras will be situated in the same horizontal row of pixels. If we rotate cameras that are setup as shown in Figure 5, until they are parallel to each other, the resulting camera setup would have epipolar lines that are corresponding to the horizontal row of pixels. This significantly simplifies stereopair tracing because it reduces the need for planar stereopair searching to searching along the horizontal line, thus reducing analysis time and noise in the measurement. If one of the cameras is considered as referent, disparities can be shown as an image whose pixel intensity represents relative distance to stereopair in second camera. Parallel configuration is not practical because of imperfection of cameras and the need for the accurate positioning (parallel setup could be obtained by carefully translating one of the cameras). The recorded image overlap directly depends on the camera baseline distance, in case of parallel cameras baseline reduction increases overlap and number of stereopairs. At the same time baseline is one of the sides of triangle defined by projection centers of each lens and the object point, so by reducing its size triangulation accuracy drops. Two sides of the triangle which join in the object point become larger then third side. Thus small error in angle reconstruction results in the large error in triangulated object point position. Baseline does not intersect with the image plane because epipolar lines are parallel to it. This can be exploited in a numerical image rectification procedure which generates a new view from the original images if images were recorded by non parallel cameras. For a non calibrated case rectification is illustrated by Figure 10b.

Epipolar lines from the original image (Figure 10a) become parallel and horizontal, as if they were recorded by parallel cameras. Rectification procedure takes into account only the relative camera orientation regardless of the measured object geometry. Procedure requires numerous interpolations in the reconstructing image stage, so it is not appropriate for active multi camera systems. Commercial systems that use two cameras in a convergent setup find stereopairs as explained in section 3.2. That procedure might require initial system calibration, which is here avoided by introduction of perpendicular projection. In the new system shape digitalization is conducted by projecting two mutually perpendicular patterns, consisting of combination of phase shift and Gray code [16], as illustrated by Figure 11. That way each correctly illuminated pixel in cameras carries information of horizontal and vertical phase. Finding stereopair is a problem of searching for the pixel with equivalent codes in the image domain. The search has to be conducted in two phase images per camera. It is simplified by knowing that projected patterns were perpendicular and direction of phase increase for each pattern is known. Analysis of search algorithms will be conducted on the assumption that perpendicular patterns were projected on a flat surface, while horizontal pixels match in the cameras used. Camera pixels have integer coordinates so the initial analysis will use only integer values. After calculation of horizontal and vertical phases from phase and Gray code images, one pixel is selected in the reference camera (usually left one), so its horizontal and vertical phases are known.

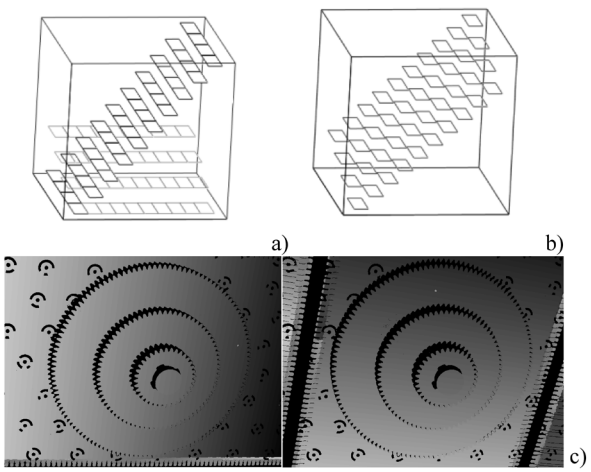

Figure 11. a) Illustration of double coding, b) sum of horizontal and vertical phase images, c) absolute phases in double coded camera 1

Slika 11. a) Ilustracija dvosmjernog kodiranja, b) zbrojene horizontalne i vertikalne faze c) apsolutne faze u dvosmjerno kodiranoj kameri 1

It is followed by a searching picture of vertical phases from the second camera, until the column with the exact vertical phase is found. Under the perpendicularity condition horizontal phase has to be positioned somewhere along the column from the vertical absolute phase image. Search procedure uses integer values because reference and target pixels are represented by integers. The procedure is repeated for all correctly coded and digitized pixels. This method can be extended so instead of looking for integer pixel, one looks for the pixel placed one row up and one column left from the selected pixel. It is now similar to object methods because a small facet consisting of four pixels is used. It allows bilinear interpolation of the non integer position of the target pixel. This is practical in the case of real cameras because they provide images that are a discretization of the actual surface. Due to the need for a certain angle between cameras (usually somewhere in the range of 20°-30°) projected patterns are not always mutually perpendicular and parallel to camera pixel rows and columns. This approach has the advantage of reducing noise in the reconstructed cloud but uses information from the neighboring pixels, thus converging towards object methods. A two-way projection reduced the need for the epipolar geometry and assigns two different phases to each image, but this method still can not be directly compared to the absolute object methods because it doesn't assign one unique ID to each pixel. It can be clearly seen if we add both phases into a unique phase, as illustrated by Figure 11b. Now the same ID (represented by height) repeats under 45° angle and additional control mechanism is needed to find the correct stereopair. In two camera systems that use pattern projection in only vertical direction, Gray code contributed to the uniqueness problem solving by unwrapping partial phase images. Resulting absolute phase image is approximately monotonous plane. Gray code did not contribute to the accuracy of the overall method. Its contribution is only in giving the exact direction for phase unwrapping. Absolute phases obtained by vertical projection are here used analogous to Gray code in two camera systems, while absolute phases projected in horizontal direction were used for recovering absolute phases. The principle will be explained on the 8bit image sample consisting of four lines, each 10 pixels wide. Let the intensity of the first pixel in a row be zero and the last 255. Due to graph clarity, phase in horizontal projection increases to the right. If a single pixel is chosen in vertical absolute phase image obtained by projecting on the flat plane (under the condition that pixels are parallel to horizontal phases), that pixel will have a phase which repeats in the vertical phase image along the selected row. That row will be used as the initial line. Relative movements during the pattern projecting are not allowed; let us now read each pixel from the horizontal phase image. This leaves us with a discrete phase distribution that looks like a small staircase line. If projected image consisted of only that line, the uniqueness problem would be automatically solved because each pixel would contain its own unique ID defined by the horizontal phase. This procedure is repeated for a next row in the vertical phase image for a pixel with first larger vertical phase value. The second line of horizontal phases is obtained. It is neighboring line from the previous stage, Figure 12a. Since those two lines consist of equal or similar horizontal phase values, but with integer difference in the vertical phases, the uniqueness problem is still not solved. It would be absolutely solved only if each pixel that both lines consist of had a unique ID that would repeat in our 20 pixels only once. The next step is to increase all vertical phases from the second line for some constant value. In case images were recorded by 8bit cameras with 256 light levels and phase images were projected with 64 light and dark stripes, largest horizontal or vertical phase expectable for a row of pixels is 256*64=16384, meaning that in that case we would have to increase each row of vertical phases by 16384+1. That step is increased by one so that the first pixel from the second row would not interfere with the last pixel from the first row. It is a minimal step needed to differentiate both lines, while in our simplified example sufficient step would be 10+1. Using any other step higher then minimal would also result in the absolute phase image. Now each pixel in two observed lines of horizontal phase images is coded by the unique code, which proves the absolute indexing possibility of a perpendicular projection technique. The advantage of this approach is the possibility of using any other projection technique that can provide two perpendicular phase images (e.g. direct perpendicular

projection of color coded lines or heterodyne pattern). If we repeat this procedure for the rest of the pixels, the resulting absolute phases in our example are shown by Figure 12b. Compared to Figure 11b, each unique code now repeats only once, and stereopair searching now can be done in a single image per camera. This procedure has to be conducted for all cameras involved. Each image can be considered as the indexed set, which associates two image coordinates to each absolute ID.

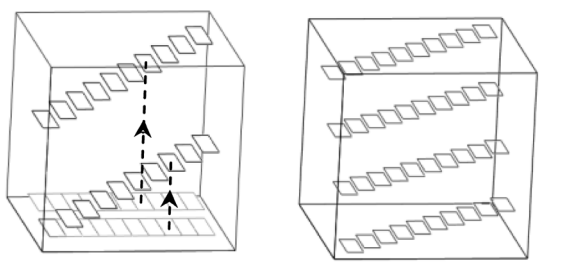

a) b)

Figure 12. Absolute phases for a) two rows of pixels, b) whole model

Slika 12. Apsolutne faze za a) dva reda piksela i za b) cijeli model

Stereopair reconstruction now can be conducted simply by converting image into the single pixel line, by adding each horizontal phase row one after the other. This approach reduces two-dimensional searching problem to one-dimensional problem. Searching for stereopairs in a one-dimensional array is faster then searching through horizontal and vertical phase images, especially because the next target index is probably the next neighbor of the previous index. The solution is a straightforward problem is observed as the intersection of two indexed sets which keep two image coordinates for each absolute ID. Finding stereopairs is now reduced to reading the same index in all of the cameras. This approach avoids the need for a reference camera, as well as for the usage of searching and sorting algorithms. The entire analysis is done by array manipulation, analyzing pixel by pixel. In order to solve our example, one would have to use one-dimensional matrices with 40 members. For the actual images consisting of e.g. 768*572 pixels, with chosen step of 16385, largest index could be 16385*16385 $\approx 2{,}7*10^8$. Due to the width of the overlapping areas resulting in projector rotation 572*572 matrix elements would suffice. If each of the 572 rows is reindexed, largest index can be in a range of 572*16385.

5. Phase image filtering

Section 3.2. describes how stereo camera systems based on a vertical pattern projection depend on the epipolar geometry for stereopair tracing. The additional uniqueness problem appears because of the projection of vertical lines, along which the same absolute phases repeats from top to bottom of the image. Discontinuities and occluded areas do not have a significant influence on the resultant point cloud because in those areas stereopair of the point visible in the reference camera could not be visible in the second camera. The pixel in the reference camera without known stereopair can be automatically rejected as bad. This provides a simple but efficient mechanism for the filtering of incorrect stereopairs. Rejection of incorrect stereopairs can be conducted even before the triangulation, which makes the overall analysis faster. Systems that use more than two cameras for point triangulation and do not depend on the epipolar geometry are more susceptible to stereopair identification errors because the correct position of object point depends on the accurately located stereopairs in all the cameras. Erroneously located stereopair in one of the cameras could lead to triangulation error and have to be eliminated after triangulation of all stereopairs is conducted. Outlier elimination in optical systems is usually conducted by comparing deviation of an object point to the overall deviation (usually points with deviation better then 3 sigma are preserved). Outlier detection can slow down the analysis because time is spent on searching for wrong stereopairs in two phase images per camera, their triangulation and afterward statistical elimination. In the case of multi camera systems based on bundle adjustment, if wrong stereopairs were not completely eliminated the system could lose convergence during the self calibrating bundle adjustment step. If the mathematical model is based solely on bundle adjustment principle, then a direct mechanism for outlier filtering similar to the epipolar principle does not exist. Epipolar principle could still be used between each camera pair but that goes against the double projection idea. In order to avoid outliers, additional controls have to be introduced in the stereopair detection stage. It would be best to reject outliers before triangulation, in a domain of horizontal and vertical phase images. If we choose to ignore errors that are a result of image digitization, most of the errors in stereopair detection can be traced back to the model surface discontinuities, and in the locations of large phase gradients.

5.1. Modulation filtering

Discontinuities filtering will be illustrated on the pyramidal model consisting of three steel gears connected by a short shaft. In the vertical phase image recorded by camera 1 (Figure 13a) discontinuities which are a result of surface gradient are painted black. On the other part of this image which shows the opposite side of the model there is a visible edge (Figure 13b), as a result

of lower surface occlusion by upper surface. This effect exists because of the angle between camera and surface normals. If one could position camera in such a way that its axis is collinear to the projector axis, phase image 13b. would look like a continuous image without the occluded areas.

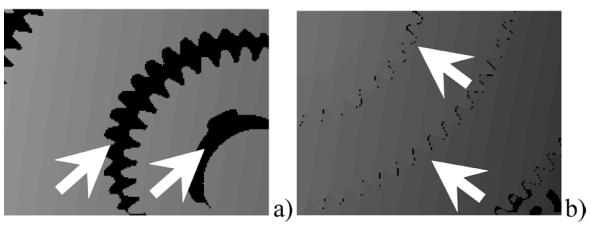

Figure 13. Discontinuities in phase images resulted by a) filtering, b) surface occlusions

Slika 13. Diskontinuiteti fazne slike nastali a)filtriranjem b) zasjenjenjem niže razine višom razinom

Let this model have white, approximately Lambertian surface properties and digitization system has no apriori knowledge of the model geometry so outlier filtering has to be conduced in the image domain. In our experiment horizontal and vertical phase images were projected, consisting of phase shift and Gray code images. Images were recorded by four 8bit cameras whose sensitivity is considered as linear in the range approximately between 20 and 230. For the correctly recorded pixels the expected mean value of the interpolated cosine curve (Figure 6b) should be around 130, while modulation should be about 100. Phase image filtering is conducted in the partial phase image before the Gray code projection. It is based on the control of modulation deviation from the expected value of sinusoidal image intensity, for a given object point. Phase filtered results will be shown on the absolute phase images. Unfiltered vertical absolute phase image are shown in Figure 14a.

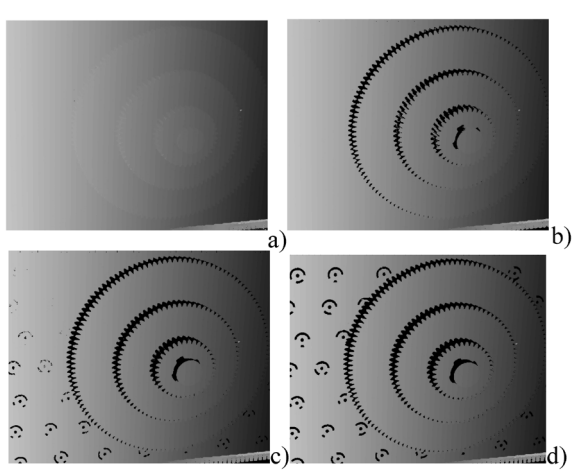

Figure 14. Modulation filtering of the absolute phase images with modulation threshold: a) 0, b) 10, c) 20, d) 30

Slika 14. Filtriranje faznih slika amplitudnom modulacijom iznosa a) 0, b) 10, c) 20, d) 30

The projector was positioned approximately perpendicular to the gear sides, its lens axis is almost collinear to the gear axis. From that position only the gear sides can be correctly illuminated and coded, the active surfaces of the gear teeth cannot be correctly illuminated because of their respective orientation. Visible tooth elimination begins in Figure 14b where pixels with modulation lower then 10 were rejected. Even if they were correctly coded, those pixels in square camera setup (Figure 1) cannot be visible in more than one camera so they can be safely discarded. Area with discontinuities increases by raising modulation threshold (Figure 14b-d). Apart from the selected threshold, the end result could also be affected by occlusions, insufficient surface preparation or because of the double reflections. Increase in discontinuities overlaps with the moment of circular hole appearance (they belong to the black coded points printed on the white base paper). Coded points were correctly filtered when magnitude was set to 30.

5.2. Gradient filtering

During the analysis stage, discontinuities can interfere with stereopair search algorithms in the additional cameras because they break the continuity of the image matrix for the observed phase gradient direction. Their influence can be avoided by introducing the additional tests that would skip dark pixels (non coded pixels are represented as black pixels in Figure 14). In that case pixels belonging to discontinuities are still affecting the analysis time as they can be found in both horizontal and vertical absolute phase images. One way to deal with this problem in two camera system is to sort vertical phase image in the second camera. By sorting the vertical phases in the horizontal direction black pixels representing holes in the phase images can be eliminated, but the original phase pixel coordinates represent the actual stereopair position so they have to be preserved in a separate array. Stereopair matching was conducted in sorted phase domain images in two steps: in the initial stage the rough stereopair search is conducted by matching horizontal and vertical phases, followed by sub pixel interpolation in phase domain. During the initial stage of locating stereopair belonging to the reference pixel in the left camera, stereopair whose phases are closest or equal to the reference pixel phases is found in the right camera at its integer coordinates, or as the first pixel up and left from the seeked pixel position. Digitization errors and local surface properties are suspected to be the cause for phase discrepancies in phase images. In order to reduce influence of the image digitization errors, in the second step result is enhanced by a bilinear interpolation in phase domain within a square 2x2 facet. The pixel found in the initial step defines the upper left pixel in a facet. Bilinear interpolation in phase domain can provide results only if

all of the phases in a facet are sequential, belonging to a continuous phase surface. This motivated the introduction of gradient phase filtering in the rest of the cameras, conducted in the neighborhood of the pixel found in the initial search step. This filter allowed us to avoid pixels in whose vicinity are phase discontinuities and large local phase gradients. For the pixels surrounding the pixel found in the initial search step we calculate mean phase value which is reduced by the actual phase in the observed pixel, eq. 8., and was used in both phase coding directions.

$$\left| \frac{1}{9} \begin{bmatrix} 1 & 1 & 1 \\ 1 & 1 & 1 \\ 1 & 1 & 1 \end{bmatrix} - \delta(x,y,t) \right| \leq 20. \quad (8)$$

Sign of the gradient carries no valuable information so we observed only the resulting absolute value. In the ideally recorded phase images of the flat plane this value theoretically should be zero, but in the real measurements 20 was found to be a sufficient threshold. Apart from the bilinear interpolation influence, sharp edges can represent a particular problem for both laser and coded light projection systems because sometimes it is impossible to correctly determine if pixel in camera correctly digitized phases of the point belonging to the edge or it also captured part of the empty space next to the edge. Gradient filtering takes into account first pixel next to the pixel on the edge of the surface, which gets rejected. Apart from the influence on search algorithm stability, it is convenient to filter edge out because of the non predictable light reflections of the projected pattern, which can locally alter phase images. Gradient filter introduction resulted in increased search algorithm stability, while also reducing number of erroneously identified stereopairs which resulted in a shorter triangulation time and better bundle adjustment convergence.

6. Image analysis strategies

6.1. 4-3-2 triangulation

Object point triangulation in a stereo camera system has to be conducted after all stereopairs in the both cameras are identified. Each pixel in the left reference camera whose stereopair is not found cannot be triangulated and is rejected as erroneous. If we apply the same principle to a system consisting of e.g. four cameras, triangulated point cloud will contain only those object points that where correctly observed and coded in all four cameras. Points that were correctly coded but were visible in any two or three cameras would be rejected as erroneous. Filtering of the results and elimination of the erroneously identified stereopairs would be conducted before the triangulation, resulting in the additional holes in measurement results (Figure 15a). The resultant point cloud would cover same, or more probably even smaller surface of the measured object compared to current commercial two camera systems. This effect is caused by the possibility that part of the measured surface which is correctly coded is occluded in some of the cameras. In that case additional cameras would not increase the overall number of scanned points per measurement, but it would result in an over determined system. If we measure a flat surface with the ideally setup system, one could expect that all stereopairs would be correctly identified in all the cameras used. Industrial products made of metals usually have non planar, arbitrarily discontinuited and highly reflexive surfaces so this approach will not satisfy demand for a fast and complete surface digitization. Since one of the goals of this work is to reduce the overall number of measurements for the arbitrary measurement object, in order to achieve additional stereopairs the analysis is conducted partially, camera by camera. Camera 1 is selected as the reference camera and stereopair tracing is conducted by some of the methods described in previous chapters. Located stereopair of the reference pixel is indexed for each of the camera separately, regardless if it was found in each of the cameras used. Pixels that were occluded in the reference camera are still not triangulated. During triangulation, apart from object points whose stereopairs were found in all of the cameras, this approach allows triangulation of points that were correctly coded in the reference and a minimum one camera, regardless of camera position. This procedure is justified because during triangulation of just two stereopairs this multi camera system reduces to the operation of current commercial two camera systems. Should there be need triangulation can always be conducted only for points visible in all of the cameras. Since projector was not calibrated, pixel in reference camera whose stereopair is not found in any of the cameras cannot be triangulated, which explains the name of this method.

Figure 15. brings detail of the digitized surface obtained by using a four camera system with a single reference camera. Only points visible in all four cameras are shown. Numbers in the image corners represent number of the correct object points in the point cloud, displayed in regards to their statistical elimination factor written in description. According to the ATOS specifications, points whose deviation is within (3-4)σ are used as valid, which in this case corresponds to the point clouds shown in Figures 15c and 15d.

If we compare completeness of the digitized surface and number of object points shown in Figure 15 with Figure 16a, even with points that are within 1σ justify the use of the 4-3-2 method. Should we use points obtained with 4-3-2 method whose deviation is better then 4σ, in this example total number of points would go to 34171, compared to 34131 points whose deviation is better then

2σ, Figure 16b.

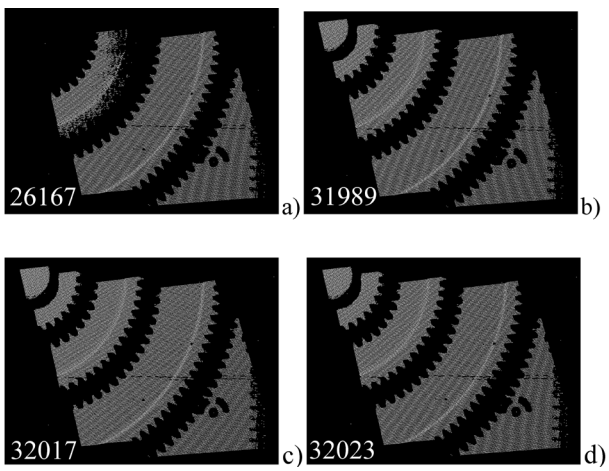

Figure 15. Point cloud of correctly coded points that were simultaneously visible in all four cameras, whose deviation was less then a) 1σ, b) 2σ, c) 3σ, d) 4σ.

Slika 15. Oblak ispravno kodiranih točaka istovremeno vidljivih u sve četiri kamere čija je devijacija triangulacije manja od a) 1σ, b) 2σ, c) 3σ, d) 4σ.

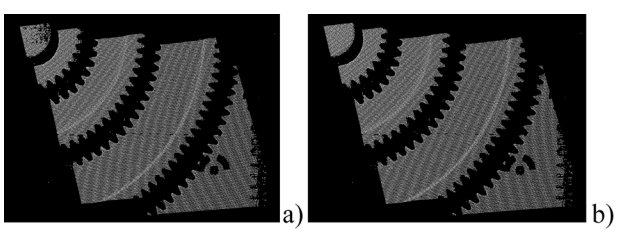

Figure 16. Point cloud triangulated with 4-3-2 method whose deviation was less then a) 1σ, b) 2σ

Slika 16. Oblak točaka trianguliran 4-3-2 metodom čija je devijacija triangulacije manja od a) 1σ, b) 2σ

6.2. Sequential (1,2,3,4) analysis

Systems that use a single reference camera will eliminate correctly coded pixels in the rest of the cameras that were not visible in the reference camera, as well as pixels visible in the reference camera but not visible in the rest of the cameras. Here we will extend definition of a reference camera by help of a four camera system, where camera 1 serves as a reference camera (Figure 1). For a short row of pixels marked with white line (Figure 17 a) stereopairs in the rest of the cameras (Figure 17 b-d) for a square camera setup were located by using chapter 4 algorithms. The projector was positioned approximately perpendicular to the gear sides. A model is chosen so that object points which were correctly coded by the projector (but were occluded in the reference camera), have to exist somewhere in a stacked gear setup. In order to illustrate this, in Figure 17a the selected row of pixels is marked by a series of vertical lines. Each line starts on the top of the Figure 17a and ends at the chosen pixel. Due to the high density of pixels in the reference camera, this visualization looks like a monochromatic, continuous square. Stereopairs belonging to object points that were found in the rest of the used cameras (Figure 17b-d) are marked in the same way. Stereopairs were identified from left to right, discontinuities are marked black.

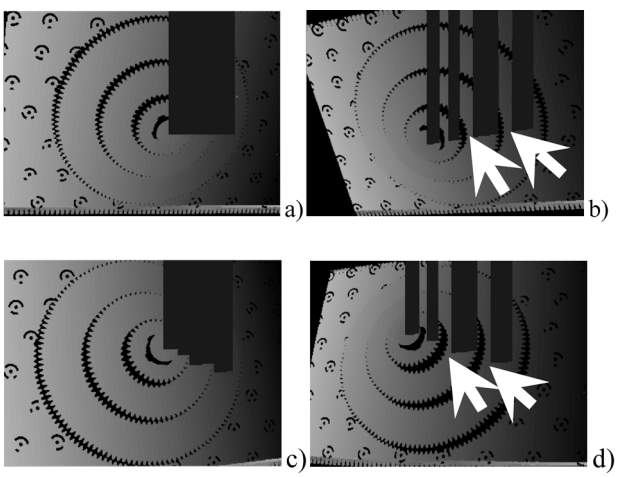

Figure 17. Illustration of stereopairs found with only one reference camera: a) reference camera, b) camera 2, c) camera 3, d) camera 4

Slika 17. Ilustracija pronađenih stereoparova s jednom referentom kamerom a) referentna kamera 1, b) kamera 2, c) kamera 3, d) kamera 4

Because of a camera tilt, seemingly horizontal and continuous row of pixels chosen in the reference camera in the rest of the cameras looks like a discontinuited sloped line. Figure 17b now contains four separate pixel lines; each line belongs to a different level of the staircase model. If we neglect group of lines that belong to stereopairs on the axial shaft surface, each of the remaining groups begins a little bit to the right from the lower edge of the upper (smaller) gear, and ends on the edge of the current gear. Displacement of the first pixel equals to the part of the surface that was visible in the current camera but occluded in the reference camera. In order to digitize points that were correctly coded but occluded in the reference camera, we search for stereopairs with the multiple reference cameras. Sequential stereopair analysis is conducted on all the cameras used, by changing the position of the reference camera. If in our example we now choose camera 2 as the reference camera, points that were not initially taken into account will now be used in triangulation model. This approach is not usable in the two camera setup without projector calibration because occluded areas will be only visible by a single camera. Points skipped in the initial step are probably visible in cameras 2 and 4 (Figure 1b and d). By adding more cameras to the system greater

surface area will be digitized in fewer projections needed. Bundle adjustment allows adding arbitrary number of cameras, allowing the system to be modified according to the measurement need. Since sequential analysis is run on the already calibrated cameras, cameras are already setup in the global coordinate system. By running sequential analysis there is no additional error in cloud positioning because. Additional advantage of this approach is that there is no need for a physical displacement of the current reference camera, as analysis it is conducted on the already recorded images.

6.3. Combined analysis

The procedure described in the previous section can be considered just a special case of a sequential analysis because each of the steps can be combined with 4-3-2 triangulation. Figure 18a illustrates sequential analysis only for points correctly visible in all the cameras, while Figure 18b brings the same analysis combined with 4-3-2 triangulation. Edges marked with arrows in Figure 18a seemingly remind of gear teeth from the upper level gear. Since there was a small space between gears in this region, the upper level teeth didn't have contact with the lower level gear side. Even if they did touch, the space between the teeth physically cannot be visible at the same time in a four camera setup with the centrally placed projector. The edge marked by arrows is actually a result of an occlusion of a lower level by the upper level gear in the reference camera, as explained by Figure 17. In the case of combined analysis, arrows in Figure 18b mark the new edge, whose detail from square area is enlarged in Figure 18c. Silhouette of the previous cloud is still visible in the enlarged part. One would expect that this new edge will look approximately as the projection of the upper level gear to the lower level, but in this example it is not the case because during the rotation and displacement of the projector it was accidentally placed in a way that upper level teeth cast shadow to the lower level gear so shape of the teeth was lost in the horizontal phase images. Combined analysis allowed digitization of more details without the need for the additional projections. Besides influencing the completeness of the surface digitization, spatial definition as well as surface detail definition is improved which are now described by four times more points compared to the single reference camera setup, as illustrated by Figure 18d.

Surface detail is shown with marked zones numbered by a number of reference cameras used. This effect is possible because integer and fine stereopair search as a result give non integer locations of stereopairs, which directly translates to the spatial position of the measured object points.

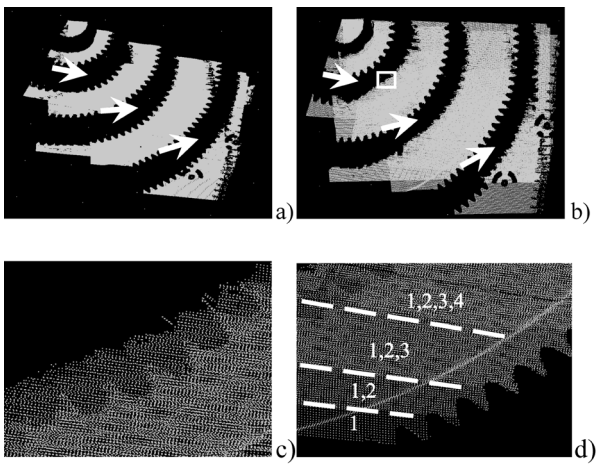

Figure 18. Point cloud as a result of a) sequential analysis, b) combined analysis, c) detail, d) spatial resolution

Slika 18. Oblak točaka kao rezultat a) slijedne analize, b) kombinirane analize, c) detalj, d) prostorna razlučivost

7. System calibration

Multi camera system calibration is here modeled as a bundle adjustment problem with the approximately known internal calibration parameters. External parameters have to be determined by the use of the additional image markers. Initial values of internal parameters are set based on the ATOS manufacturer's datasheets, for a given camera and lens focal length. They are optimized during the calibration process. External parameters are unknown and have to be determined by the bundle adjustment method assisted by the passive markers. Passive markers on the calibration object are necessary in order to solve the uniqueness problem in the domain of calibration images (taken without projecting patterns). For that purpose we used coded points. We choose black circular points on the white surface surrounded by a dark ring divided in 10 parts, whose combination allows the automatic and unique recognition of 100 different point codes. A code is only used for stereopair recognition and does not carry additional measurement information. For each of the four cameras five calibration images were recorded. Four of them were recorded by camera placed perpendicularly to the calibration panel that was sequentially rotated by 90° around the axis perpendicular to the panel, approximately parallel to the lens optical axis. the last image was recorded from a displaced and tilted camera position that will be used later for recording of projected pattern. the outer camera orientation parameters were set based on user experience, in a way that each of the cameras sees the whole projected area with the most coded points possible. All presented experiments were conducted with the identical Sony XC-75CE cameras equipped with two lens pairs: cameras 1 and 2 had Schneider c-mount 12.5mm lens, cameras 3 and 4 had 12mm lens. The effect

of number of cameras on the internal camera parameters (camera constant, principal point coordinates and their deviations) was analyzed, table 1. Planar and spatial free-form calibration objects were used. For a given calibration object, calibration procedure was conducted in three steps: in a first step two cameras were calibrated (cameras 1 and 2 are the first camera pair), in the next steps cameras 3 and 4 were added to the model. System calibration starts with the following values of the camera constant: for a chosen camera and 12.5 mm lens camera constant equals 1470.59 pixels, while for a 12 mm lens equals 1411.76 pixels. Principal point is assumed to be in the center of the CCD chip. Due to the similarities in camera pairs, it can be expected that final internal parameters obtained after the bundle adjustment will be similar within pairs, and larger for the first pair. Position of the principle point depends on the accuracy of lens and camera production, it should line near the center of the image.

7.1. Planar calibration object

Standard commercial Atos systems use planar calibration object for a camera calibration, in the first experiment we chose planar marked panel to be used for the assessment of effects that adding additional cameras have on the internal orientation parameters of the calibration model. Calibration results are shown in Table 1. Coded points whose diameter was chosen to be 4mm were printed with ink-jet printer with 1200 dpi resolution on a self-adhesive white paper and attached to a rigid panel. A panel is fixed in the horizontal plane and recorded by four cameras in the convergent square setup (Figure 1). If we compare the calibrated camera constant c for cameras 1 and 2, in all three calibration scenarios for camera 1 converges to 1510pixels, while camera 2 converges to 1549 pixels. Considering only calibration of two cameras, where camera constant for camera 1 was 1346 pixels, its obvious that there has to be some additional influence on camera 1 whose influence is minimized by adding the additional cameras, but it can't be explained based on the measured numbers. After careful observations of lenses used in camera 1 (after all the experiments were conducted) it was determined that some of the lenses inside lens 1 were loose. It was apparent that after the lens was taken off the camera and shaken, a clicking noise could be heard.

Convergence speed is faster for camera 2. If we used those two cameras in a two camera setup there would be a considerable difference in camera constants even though cameras and lenses were the same. At the same time camera constant deviations were between 2 and 4 pixels, and considerably jumped by the addition of third camera. As we added more cameras to the system this deviation stabilized and was in the same range of magnitude for all the cameras used. Because of the design of the experiment, for cameras 3 and 4 there is less data available, but convergence is considerably faster and there is better overlap in the final value: 1473 pixels in 3 vs. 1486 pixels in camera 4. Final deviations are comparable between pairs, even if we compare left camera pairs (cameras 1 and 3) with the right camera pair. Camera parameters, their orientation and light conditions can affect the internal camera parameters, which makes it hard to predict the principal point locations. It can be assumed that there would have to be some regularity in the principal point position deviation, regarding their order of magnitude. If we neglect the first camera pair where those deviations were considerably smaller than in the rest of the cases, it is visible that by adding the additional cameras there is a tendency of deviation reduction. There were 100 pixels per mm on the camera chip, so largest principal point displacements in the four camera case were in the range of 0.3 mm off of CCD chip center point.

Table 1. Internal camera parameters for planar calibration object, pixels

Tablica 1. Unutrašnji parametri za slučaj kalibracije planarnim kalibrom, pikseli

Camera / Kamera	Cam. ID / Broj	c	σ_c	x_H	σ_{xH}	y_H	σ_{yH}
1	2	1346	2,8	25,8	1,4	18,2	1,2
	3	1497	19,9	-8,1	6,0	24,8	8,8
	4	1510	18,4	-5,2	5,6	18,6	8,2
2	2	1583	4,0	64,6	1,8	-77	1,6
	3	1558	21,6	-39	8,0	-14	11
	4	1549	21,2	-36	7,8	-11	11
3	3	1477	18,9	12,6	7,2	-14	5,1
	4	1473	17,2	11,7	6,5	-14	4,6
4	4	1486	23,1	0,5	9,7	-2,1	11

7.2. Spatial calibration object

Every object point whose index is obtained by a double projection can be considered as a valid coded point, meaning that the entire surface of the measured object can be used as a free-form spatial calibration object. This experiment will be limited to free-form calibration objects defined by a discrete coded points, symmetrically distributed on the volume of the pyramidal object. Symmetry in the point distribution leads to simplification of the calibration planning, and at the same time provided the uniform point distribution in the recorded images. Besides nine coded points on the model, there were additional points placed on a panel holding the model. Calibration was conducted in a same way as in the previous chapter, with the same equipment and measurement volume, taking special care not to alter internal lens parameters while handling the cameras.

Table 2. Internal camera parameters for free-form calibration object, pixels

Tablica 2. Unutrašnji parametri za slučaj kalibracije prostornim kalibrom, pikseli

Camera / Kamera	Cam. ID / Broj	c	σ_c	x_H	σ_{xH}	y_H	σ_{yH}
1	2	1387	5,3	25,9	2,6	15	2,5
	3	1507	11	-0,3	3,5	15	5,1
	4	1524	8,8	4,2	3,0	7,1	4,2
2	2	1537	11	62,7	3,5	-61	3,3
	3	1511	7,8	-18,8	2,5	4,9	2,5
	4	1532	5,7	-23,9	2,0	0,5	2,0
3	3	1454	10	6,3	4,0	-20	2,8
	4	1470	7,8	11,8	3,1	-16	2,2
4	4	1469	4,5	8,7	2,1	-7,8	2,1

In the case of two camera calibration, camera constants behave in a similar way (Table 2) as in the case of planar calibration object. By adding cameras 3 and 4 camera constants of cameras 1 and 2 considerably converge, compared to the previous experiment. The influence of a free-form calibration object is even more apparent in cameras 3 and 4, where in the last experiments constants vary only a little over one pixel. If we neglect the first camera pair, deviation of camera constant in this experiment reduces with the addition of new cameras, two to five orders of magnitude lower then in the first experiment. For the principal point position the same limitations apply as in the previous chapter. Measured data here also do not show tendency to converge towards the image center. However, principal point deviations are considerably smaller and more unified compared to the previous experiment, ranging from 2 to 4 pixels. Both conducted experiments show the existence of the influence of the calibration point distribution and number of cameras on the internal camera parameters. Deviations of all the observed values are consistently smaller in case of the free-form spatial calibration object.

7.3. Spatial calibration object with displaced camera

In order to test the stability of the spatial calibration, by taking care not to disturb internal camera parameters, we displaced camera 2 approximately 100 mm towards the imagined center of the square four camera system. Calibration was conducted as explained at the beginning of chapter 7. Resulting internal parameter values are presented in Table 3. Compared to the experiment in section 7.2 there is a good agreement of internal camera calibration values, pair wise convergence of camera constants is especially visible for cameras 3 and 4. Deviations of camera constants are also comparable to the previous experiment, and an analogy can be drawn for the principal point deviations.

Table 3. Internal camera parameters for free-form calibration object and displaced camera 1, pixels

Tablica 3. Unutrašnji parametri za slučaj kalibracije slobodnim kalibrom i pomaknutom kamerom 1, pikseli

Camera / Kamera	Cam. ID / Broj	c	σ_c	x_H	σ_{xH}	y_H	σ_{yH}
1	4	1521	9,1	2,7	3,1	10,70	4,4
2		1538	5,6	-29,7	2,1	-0,2	1,8
3		1458	8,1	7,8	3,2	-18,9	2,2
4		1458	4,6	14,8	2,0	-11,2	2,1

Conducted experiments show that by using a free-form spatial calibration object there is a measurable influence on the internal camera calibration parameters, which directly relates to the quality of the digitized results of the measurement that follow calibration. Even though camera lenses were fixed, the internal camera parameters were not absolutely constant. By changing external camera parameters there was also change of the internal parameter change, but by using spatial calibration object this influence is significantly reduced.

8. Experiments

Specimens used in our tests were chosen to illustrate boundary cases that can be seen in the actual measurement praxis. Continuous flat plate represents the most favorable case for the projection method digitization. Surface normals are mutually parallel, projector can be oriented in a way that projector axis is approximately perpendicular to the surface (surface is treated with titanium oxide powder so it exhibits Lambertian properties). That way geometry of the model does not cause considerable distortions of the projected pattern, all cameras can be setup to see the entire projected pattern and phase images do not have discontinuities or occluded areas. Since goal of this work was to develop a flexible multi camera system that can digitize arbitrary geometrical shapes, it was necessary to design experiments that will allow testing the analysis algorithms presented in previous chapters. Instead of flat plane digitization we chose to digitize pyramidal form with uniaxial symmetry, Figure 19. It consists of mutually separated gears with approximately planar sides. We used three straight cut gears that formed measurement volume of 200x200x60 mm. The added benefit of our model is that edges of the each stair are additionally discontinuited. They represent zones where secondary reflections might cause additional errors in measurements. If we neglect small local curvatures in a zone near the teeth, normals of this model are also parallel, but compared to flat plane this model has spatial discontinuities. This object is already been discussed in previous chapters where it was used as illustration of each method.

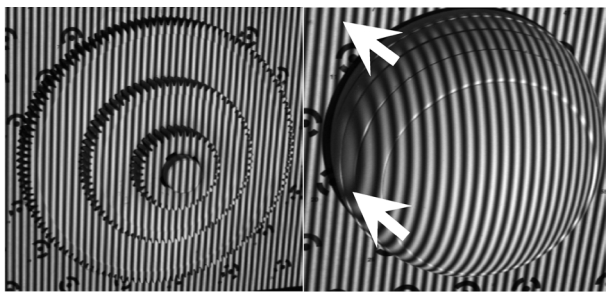

Figure 19. Comparison of the measured objects

Slika 19. Usporedba mjernih objekata

Spherical model represents another extreme case for the optical digitization systems because apart from a small number of normals that are approximately parallel to the projector axis, sphere has a large number of normals that intersect in the sphere center and are pointed in all directions in space. It is safe to say that no optical system with a single projector can digitize sphere with a single projection, because all the points on the surface cannot be correctly illuminated by a single projection. Because of symmetry, we used part of the polymer sphere with 120mm diameter. Since the projector projected a pattern with sinusoidal light intensity distribution (without sharp edges between dark and white lines), based on the image observation it is impossible to evaluate loss of sharpness of the projected pattern in regards to the position on the sphere surface. The width of the projected lines will be smallest in the point to which projector is directly perpendicular, and it will grow as the sphere normal angle increases, perpendicular to the projected lines. This effect is strongest on the outer sides of the model (same projected line is marked with arrows in Figure 19). As the surface normal angle increases (compared to the angle of the projected light) the possibility for surface digitization decreases. In order to make point cloud visualizations clearer, we decided to show only every third triangulated points in Figures 20 and 21. The sphere consists of 8 separable elements, 5 of them were used in setup shown in Figure 19. The transition zone between elements is not smooth; a small step is visible in Figure 19. The largest top element covers half of the top of the sphere (closes 45° angle regarding the axis of symmetry). The surface of other elements has a normal angle larger then 45° which make them very difficult to scan because most of the light reflects away from the sensor and model occludes that surface. On the surface of the sphere there is no point belonging to elements 2, 3 and 4 that can be visible in all four cameras in a square setup. The projected pattern completely covers surface of the top element, which is almost completely visible in all of the cameras.

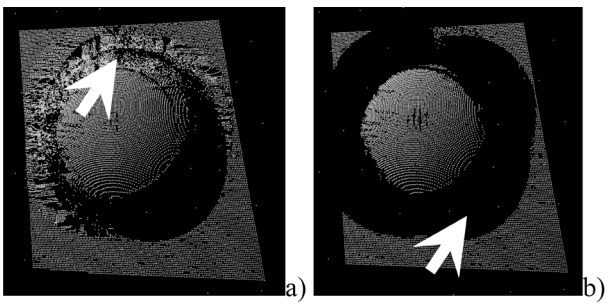

a) b)

Figure 20. Triangulation of points visible in all four cameras with deviation better then 4σ and gradients less then a) 20000, b)20

Slika 20. Triangulirane su samo one točke koje su vidljive u sve četiri kamere s devijacijom 4σ i gradijentom a) 20000, b)20

Should we triangulate only points that were correctly coded in all the cameras, only in element 1 zone can exist points in a point cloud, Figure 20. As initially expected, the zone belonging to element 1 is for both filtering methods digitized almost completely. Non filtered point cloud (Figure 20a) contains part of the element 2 (marked with arrow), but with visible noise and irregular point distribution in space. Except for the sphere surface, part of the fixturing plate is also visible. For each of the cameras part of the fixture surface is occluded by the model, but it is almost entirely correctly coded by projector. In the case of triangulation of points correctly visible in all four cameras, in the occluded areas shouldn't exist in measured results. Point cloud on the flat fixture plate obtained by gradient filtering (Figure 20b) agrees with this assumption. The black area without measured data is located on the occluded areas behind the model. It contains four circular parts whose shape agrees with the spherical objects shape. Non-filtered point cloud (Figure 20a) contains measured results even in the fixture zone; occluded zone is correctly defined only in a zone occluded in the reference camera. If we repeat analysis by 4-3-2 triangulation number of triangulated points on the model and on the surface should increase (Figure 21). In the image of filtered model (Figure 21b) upper arrow marks the surface area that belongs to element 2, which was visible in cameras 1 and 2. This zone is larger for non filtered point cloud, but with considerable amount of noise. Fixture zone now has better definition, compared to Figure 20b, because triangulation is carried out for points that were visible in the reference and at least one other camera. The black zone without results, marked by lower arrow, was not visible in the reference camera and is thus skipped in the analysis even though it was visible in the rest of the cameras. We also carried out the combined analysis on the original phase images, results for points whose deviation is better then 4σ and 1σ are shown in Figure 22.

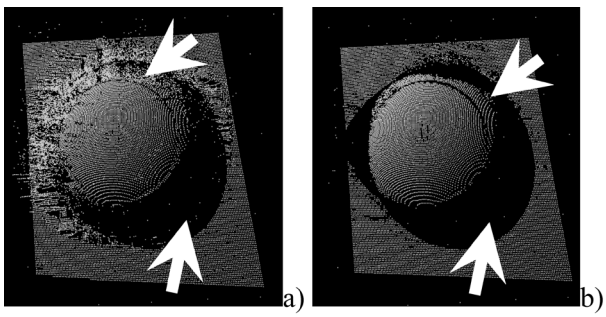

Figure 21. 4-3-2 triangulation with 4σ deviation and gradients less then a) 20000, b)20

Slika 21. Triangulacija 4-3-2 postupkom s devijacijom 4σ i gradijentom a) 20000, b)20

Point clouds were triangulated on the filtered phase images with step 20, because of the fourfold increase in number of points Figure 22 displays only every fifth point. Sequential analysis improved completeness of digitization of the fixture, compared to previous experiments. Remaining black areas (marked with left arrow) were not visible in at least two cameras, or their stereopairs could not be correctly found. Digitization of element 1 is complete. Surface of the element 2 is also more defined, which is especially visible in zone that was not visible in the camera 1 (marked with the right arrow). Measurement noise is more noticeable than in previous cases, but is contained to areas where considerable deformation of projected phase lines was visible.

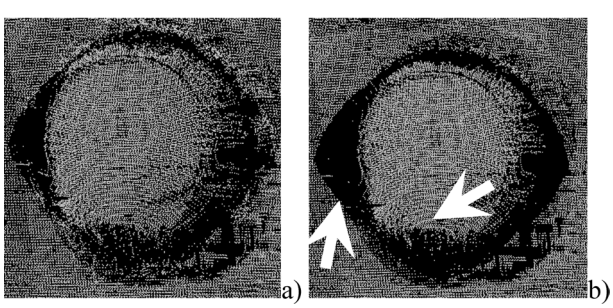

Figure 22. Points triangulated by combination of sequential analysis and 4-3-2 procedure. Shown are points whose triangulation deviation was better then a) 4σ, b) 1σ.

Slika 22. Triangulacija kombinacijom 1,2,3,4 analize i 4-3-2 triangulacije za točke čija je devijacija triangulacije manja od a) 4σ, b) 1σ.

9. Conclusion

The presented multi-camera surface digitization system allows the active digitization of general surfaces by using arbitrary number of cameras, without the need for a projector calibration. The mathematical model is based on the bundle adjustment principle, exhibits self calibration properties and allows variation of external calibration parameters. By increasing the numbers of cameras, the mathematical model becomes over determined and has the possibility of improving the initial calibration. Free form spatial calibration is introduced, whose beneficial effects on the internal parameters of the calibration model is demonstrated experimentally. The new system treats measurement object as the calibration object, resulting in improved spatial system calibration. With the introduced operator for the absolute uniqueness problem solving, each object point is indexed by a unique index. The operator can be applied to the uniqueness problem solving regardless of the projected pattern, under the condition that their projection defines two perpendicular sloped planes. Gradient filtering together with amplitude phase image filtering eliminated critical areas in phase images and thus reduced outliers before the triangulation procedure. 4-2-3 triangulation procedure enabled digitization of points that were not visible in all of the cameras, but were correctly coded. The introduction of the sequential analysis in combination with 4-3-2 triangulation for a given camera increased the overall spatial resolution and detailed definition. It affected the measurement planning process by reducing the number of needed projections on the same measurement area compared to single and two camera systems.

REFERENCES

[1] MARIČIĆ, S.; PERINIĆ, M.; ZAMARIN, A.: *An Economic and Visual System for Position Check*, Strojarstvo 50(3), 161-168, 2008.

[2] SADLO, F.; WEYRICH, T.; PEIKERT, R.; GROSS, M.: *A Practical Structured Light Acquisition System for Point-Based Geometry and Texture*, Proceedings of Eurographics Symposium on Point-Based Graphics 2005, pp. 89-98, Stony Brook, USA, 2005.

[3] ZHANG, S.; HUANG, P. S.: *Novel Method for Structured Light System Calibration*, Opt. Eng., Vol. 45, No. 8, pp. 083601-1-8, 2006.

[4] AGGARWAL, M.; AHUJA, N.: *Estimating Sensor Orientation in Cameras*, 15th International Conference on Pattern Recognition (ICPR'00) - Volume 1, pp. 896-899, Barcelona, 2000.

[5] ZHANG, Z.: *Camera calibration with one-dimensional objects*, Transactions on Pattern Analysis and Machine Intelligence, Volume: 26, Issue: 7, pages 892- 899, July 2004.

[6] IKEDA, Y.; MORIMOTO, Y.; FUJIGAKI, M.; YONEYAMA, S.: *Absolute Phase Analysis Method for 3D Surface Profilometry Using Frequency Modulated Grating*, Optical Engineering, Vol. 42, No. 5,1249-1256, 2003.

[7] YOUNG KIM, M.; CHO, H.: *An active trinocular vision system for sensing mobile robot navigation environments*, Sensors and Actuators A 125, pages192–209,2006.

[8] SUN, J.; ZHANG, G.; WEI, Z.; ZHOU, F.: *Large 3D free surface measurement using a mobile coded light-based stereo vision system*, Sensors and actuators, vol. 132, no2, pp. 460-471, 2006.

[9] SONG, L. M.; WANG, M. P.; LU, L.; HUAN, H. J.: *High precision camera calibration in vision measurement*, Optics & Laser TechnologyVolume 39, Issue 7,Pages 1413-1420,October 2007.

[10] LUCCHESE, L.: *Geometric calibration of digital cameras through multi-view rectification*, Image and Vision ComputingVolume 23, Issue 5, Pages 517-539,1 May 2005.

[11] BRENNER, C.; BÖHM, J.; GÜHRING, J.: *Photogrammetric calibration and accuracy evaluation of a cross-pattern stripe projector*, SPIE Videometrics VI', Vol. 3641, 1999.

[12] GÜHRING, J.; BRENNER, C.; BÖHM, J.; FRITSCH D.: *Data processing and calibration of a cross-pattern stripe projector*, ISPRS Congress 2000, IAPRS 33(5), Amsterdam, Netherlands, 2000.

[13] JECIĆ, S.; DRVAR, N.: *The assessment of structured light and laser scanning methods in 3D shape measurements*, Proceedings of the 4th International Congress of Croatian Society of Mechanics, Bizovac, Hrvatska, 237-244, 2003.

[14] JECIĆ, S.; DRVAR, N.: *3D shape measurement influencing factors*, Matest 2004, Zagreb, 2004.

[15] GOMERČIĆ, M.: *Doprinos automatskoj obradi optičkog efekta u eksperimentalnoj analizi naprezanja*, doktorska disertacija, FSB Zagreb, 1999.

[16] DRVAR, N.: *Optički postupak digitalizacije oblika projiciranjem kodiranog svjetla*, doktorska disertacija, FSB Zagreb, 2007.

[17] GOMERČIĆ, M.; JECIĆ, S.: *A New Self-Calibrating Optical Method For 3d-Shape Measurement*, 17th Symposium "Danubia-Adria" on Experimental Methods in Solid Mechanics, Prag, 2000.

[18] GRUEN, A.; HUANG, T. S.: *Calibration and Orientation of Cameras in Computer Vision*, Springer Series in Information Sciences, Germany, 2001.

[19] HABIB, A.F.; MORGAN, M.; LEE, Y.-R.: *Bundle Adjustment with Self-Calibration Using Straight Lines*, The Photogrammetric Record 17 (100), 635–650, 2002.

[20] SALVI, J.; ARMANGUE, X.; BATLLE, J.*: A comparative review of camera calibrating methods with accuracy evaluation*, Pattern Recognition 35, 1617-1635, 2002.

[21] GUBELJAK, N.; SEMENSKI, D.; DRVAR, N.; PREDAN, J.; KOZAK, D.; OBLAK, M.; *Object grating method application in strain determination on CTOD tests*, Strain, May 2006, Vol. 42, Iss. 2, 81-87.

[22] SALVI, J.; PAGES, J.; BATLLE, J.: *Pattern Codification Strategies in Structured Light Systems*, Pattern Recognition 37(4), pp. 827-849, April 2004.